Structure and photoluminescence properties of ZnO microrods

Dongxu Zhao, Yichun Liu, Dezhen Shen, Youming Lu, Ligong Zhang et al.

Citation: J. Appl. Phys. **94**, 5605 (2003); doi: 10.1063/1.1615703
View online: http://dx.doi.org/10.1063/1.1615703
View Table of Contents: http://jap.aip.org/resource/1/JAPIAU/v94/i9
Published by the American Institute of Physics.

Structure and photoluminescence properties of ZnO microrods

Dongxu Zhao, Yichun Liu,[a] Dezhen Shen, Youming Lu, Ligong Zhang, and Xiwu Fan
Key Laboratory of Excited State Processes, Changchun Institute of Optics, Fine Mechanics and Physics, Chinese Academy of Sciences, 140-Ren Min Street, Changchun, 130022, People's Republic of China

(Received 16 May 2003; accepted 13 August 2003)

ZnO microrods (whiskers) were fabricated by a simple thermal oxidation method. The morphologies of the samples were detected by the scanning electron microscope, which showed the ZnO microrods were about 30 μm long with a diameter of 1–2 μm. In the photoluminescence (PL) spectra, only the exciton related emission bands in the ultraviolet region could be obtained at room temperature. And, a new emission band due to the exciton–exciton collision process was observed at the low energy side of the free exciton emission under the excitation intensity of 2.1 kW/cm^2. This emission band increased nonlinearly. When the excitation intensity was increased above 16 kW/cm^2 some fine structures could also be seen clearly in the PL spectra. These fine structures originated from the cavity modes of the Fabry–Pérot étalon. © *2003 American Institute of Physics.*
[DOI: 10.1063/1.1615703]

I. INTRODUCTION

In recent years, wide-band-gap semiconductor compounds have attracted a great deal of attention because of the intense commercial interest in developing practical short-wavelength semiconductor diode lasers for the huge market needs. In this regard, ZnO is a promising material. It has a room temperature band gap of 3.37 eV, and the exciton binding energy of 60 meV should ensure excitonic survival well above room temperature (RT). Ultraviolet (UV) stimulated emission has been extensively studied in bulk ZnO crystals at cryogenic temperatures,[1–4] but observation of lasing at RT was mentioned only briefly in the works of Klingshirn[4] and in very recent reports.[5–9]

The current study in ZnO is mainly focused on the ultraviolet lasing action in disordered particles[10–12] and ordered arrays of hexagonal microcrystallite films.[5–9] The mechanism of laser emission of ZnO thin films is believed to be exciton–exciton scattering at intermediate intensity excitation (about 240 kW/cm^2), however, it may switch to electron–hole plasma emission at high intensity excitation (about 1 MW/cm^2).[5–9] To obtain an optical pumping laser with a low threshold, low-dimensional ZnO nanowire nanolasers have been fabricated,[13,14] in which quantum size effects yield a substantial density of states at the band edges and enhance radiative recombination due to carrier confinement. The use of semiconductor quantum well structures as low-threshold optical gain media was also achieved in the ZnO/MgZnO system.[15,16] But, there are few works concerned about the photoluminescence properties of ZnO whiskers.

ZnO microrods were fabricated by using a simple thermal oxidation method. The morphologies of the ZnO rods were detected by scanning electronic microscopy (SEM), which showed that the average size of the microrod was 30 μm long with a diameter of 10 μm. The emission due to the exciton–exciton interaction process was observed on ZnO rods at room temperature under very low excitation intensity (from 2.1 to 28.3 kW/cm^2).

II. EXPERIMENT

The reaction to form ZnO microrods was carried out in a conventional tube furnace with a horizontal quartz glass tube. First, the furnace was heated up to 800 °C. Then, metal zinc grains (6 N, 2 mm wide) with a quartz boat were loaded into the center of the quartz tube. The tube was heated to 1000 °C at a rate of 5 °C/min. After that, the quartz tube was kept constant at 1000 °C for 60 min under an O_2 (5 N) ambient with a flow of about 50 cm^3/min. Finally, the quartz boat was pulled out from the tube furnace when the temperature was cooled naturally to 700 °C. A white and fluffy product was obtained.

In photoluminescence, the excitation source was a continuous wave He–Cd laser with a photon energy of 3.82 eV and a power of 50 mW. The luminescence signals were detected using a JY 63 microlaser Raman spectrometer in a backscattering geometry configuration, and a charge-coupled-device camera with high resolution was used to detect the emission spectra. The excitation laser beam is focused by a lens ($\times$10 UV) to form a light spot with a 15 μm diam on the sample. The excitation intensity at the focus is 28.3 kW/cm^2.

III. RESULTS AND DISCUSSION

Figure 1 shows the x-ray diffraction (XRD) pattern of the sample. All the diffractive peaks belong to the typical ZnO wurtzite structure, which indicates that the sample is polycrystalline. The morphologies of the samples were observed by SEM, which is shown in Fig. 2. It can be seen in Fig. 2(a) that straight microrods with diameters of about several microns are grown on a porous surface. The length of the rods is more than 30 μm. The longest one is about 3 mm long with a 25 μm diam. Figure 2(b) shows a magnified

[a]Author to whom correspondence should be addressed; electronic mail: ycliu@nenu.edu.cn

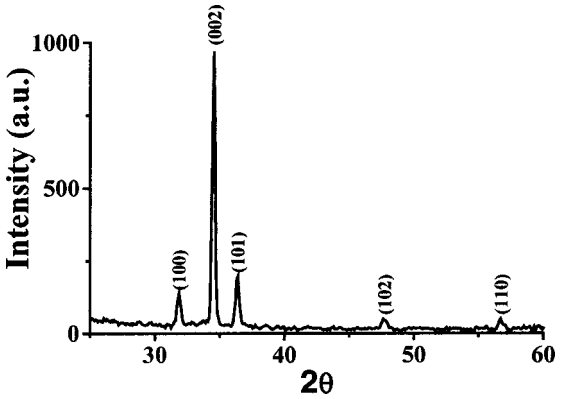

FIG. 1. XRD spectrum of the ZnO microrod.

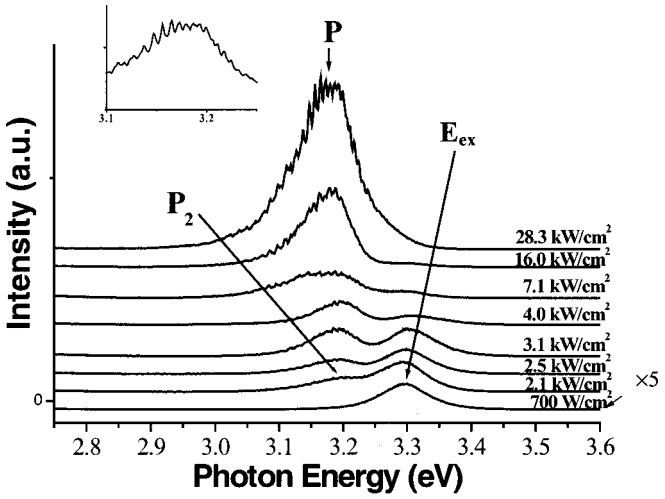

FIG. 3. PL spectra of ZnO microrods under different excitation intensities at room temperature. Inset shows the fine structure of the PL spectrum excited at 28.3 kW/cm^2.

image of the microrods. No fine structures are found on the surface of rods by high-resolution field emission SEM (not shown).

The photoluminescence (PL) spectra of the ZnO microrods excited under different excitation intensities at room temperature are shown in Fig. 3. The excitation intensity increases from 700 W/cm^2 to 28.3 kW/cm^2. At low excitation intensity there is only one emission peak (denoted by E_{ex}) in the UV region in the spectra, which is considered to originate from the radiative recombination of free excitons.[6] When the excitation intensity is increased to 2.1 kW/cm^2, a new emission band (denoted by P_2) at the shoulder of the E_{ex} band appears at an energy that is about 70 meV below the E_{ex} band. With further increasing the excitation intensity the P band grows superlinearly and finally dominates the PL spectra when the excitation intensity exceeds 16 kW/cm^2. And, the difference between the E_{ex} and P bands is broadened to about 100 meV.

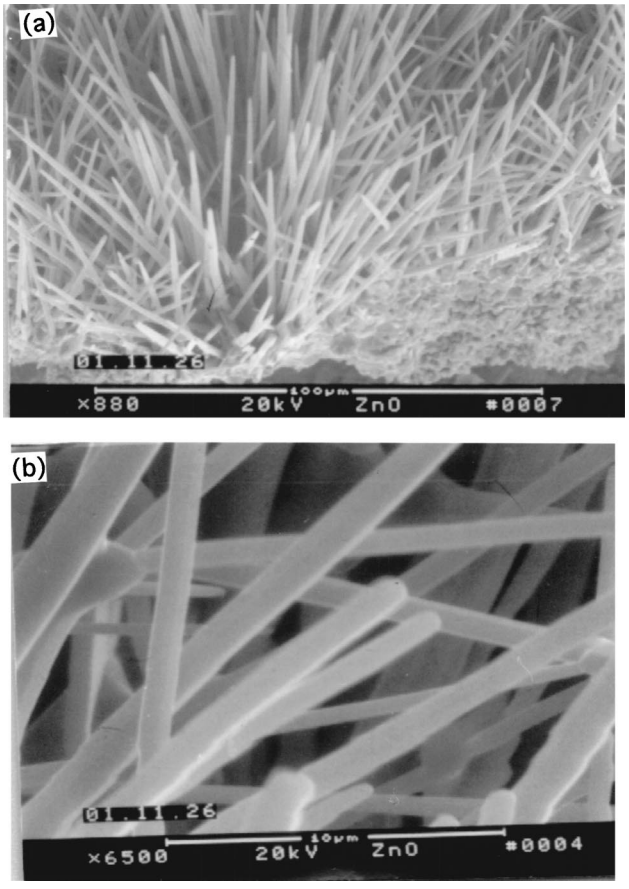

FIG. 2. SEM images of the samples.

The room temperature dependence of the integrated intensity of the P and E_{ex} bands on the excitation intensity is shown in Fig. 4(a). A competition process of the P and E_{ex} bands is clearly seen in Figs. 3 and Fig. 4(a) at low excitation intensity. At first, the integrated intensity of the E_{ex} band grows fast, then decreases gradually with increasing excitation energy. And, to the P band there is a threshold in the spectra. Under this excitation energy the emission intensity remains almost constant. When exceeding this point the P band emission intensity increases superlinearly. The slope of this rise section of the P band is 2.18, as given in Fig. 4(a). This means the intensity of the P band increases quadratically with the excitation intensity, which is consistent with the fact that two excitons are involved in the radiative recombination process.

The peak positions of P and E_{ex} bands as a function of the excitation intensity are shown in Fig. 4(b). Because of the exciton-band filling effect the E_{ex} emission peak is blueshifted with increasing the excitation intensity. And the P band is also transferred to the higher energy position. The energy difference between the P and E_{ex} bands is 70 meV at an excitation intensity of 2.1 kW/cm^2. Then, it almost remains constant at about 100 meV with increasing excitation intensity. The peak positions of the P_2 and P bands are in agreement with the radiative recombination energy, as expected from the exciton–exciton scattering process, in which one of the two excitons takes energy from the other and scatters into a higher exciton state with a quantum number $n>1$, while the other recombines radiatively. The photons emitted in this process have the energies of E_n given by

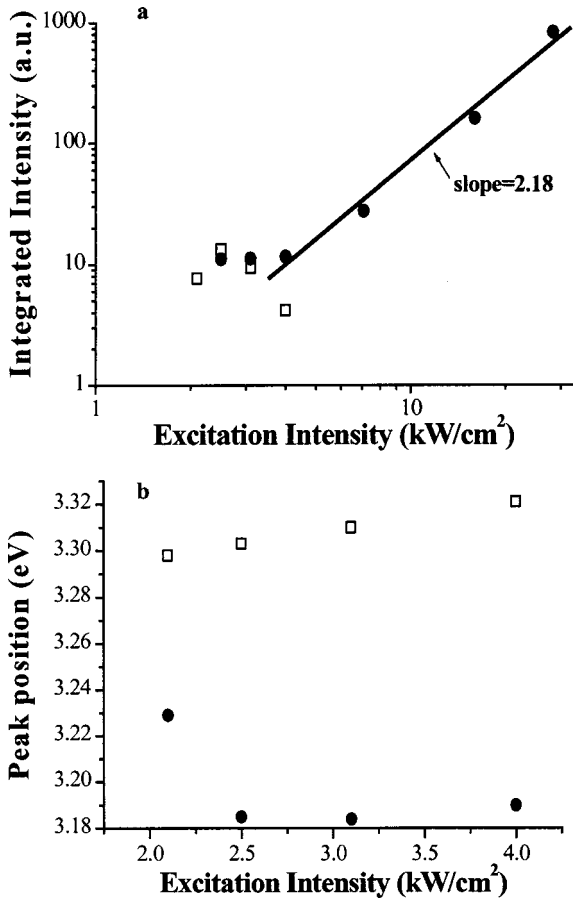

FIG. 4. (a) Room temperature dependence of the integrated intensity of the *P* band on the excitation intensity. (b) Peak position of *P* (filled circle) and E_{ex} (open square) bands as a function of excitation intensity.

$$E_n = E_{ex} - E_b^{ex}\left(1 - \frac{1}{n^2}\right) - \frac{3}{2}kT \quad (n = 2,3,4,...,\infty), \qquad (1)$$

where E_{ex} is the free-exciton emission energy, $E_b^{ex} = 60$ meV is the binding energy of the free exciton, n is the quantum number of the envelope function, and kT is the thermal energy.[4] At RT, Eq. (1) gives 83 and 98 meV for the energy difference between E_{ex} and E_2, E_∞, respectively. And, because more and more excitons scatter into higher exciton states ($n = 2,3,4,...$), the *P* band becomes a mixing of the radiative transition of excitons at different excited states. The energy difference between excitons at different excited states is very little, so the PL emission curve is continuous. And, the full width at half maximum of the *P* band grows relatively broad.

The rate of spontaneous emission of the *P* band is given by

$$\omega_{e,spont} = AN_{l,K}N_{l,K'}(N_{n,K+K'} + 1) \approx AN_{l,K}N_{l,K'} \qquad (2)$$

where $N_{n,K}$ is the density of excitons in their respective states, $A = A(n,K,K')$ is a factor containing the optical matrix element and the last expression is valid for $N_{n,K+K'} \ll 1$.[17] Equation (2) shows the quadratic dependence of the spontaneous emission on the exciton density, which is in agreement with the experiment, as shown in Fig. 4(a). With increasing the excitation intensity, the exciton density grows proportionately. As a result, the emission intensity of the free exciton increases simultaneously. When the exciton density reaches a certain value, an exciton–exciton collision occurs. It is an inelastic scattering process between two free excitons in their ground state ($n = 1$). One exciton is scattered into a photon-like state giving a luminescence photon while the other is scattered into higher excited states, $n = 2,3,...,\infty$. This process leads to a decrease of free excitons at the ground state ($n = 1$) radiative recombination. Because the scattering process between two free excitons becomes very strong, the emission intensity of the E_{ex} band is reduced. Ultimately, the E_{ex} band disappears and the *P* band is dominant in the spectra. Comparing with other references,[5,6,8] we obtained the *P* band emission with low excitation energy intensity. This is mainly because for ZnO thin films the exciton distribution is mainly in a two-dimensions region. But, for ZnO microrods the exciton is of a three-dimensions distribution. So, the probability of an exciton–exciton collision in the ZnO rod is larger than in the thin films, which induced the excitation energy density to occur in the *P* band emission of ZnO, which is lower in the microrods than in the thin films.

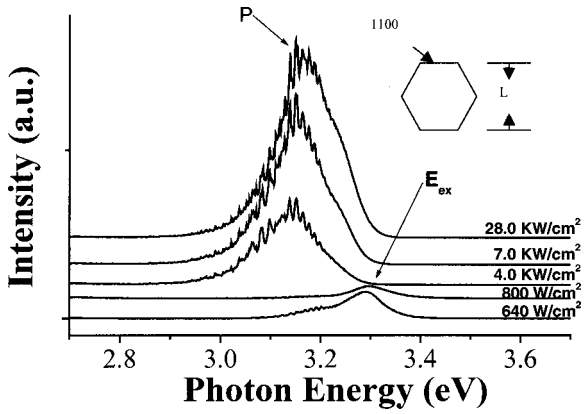

FIG. 5. PL spectra of a ZnO single rod with a 25 μm diam excited under different excitation densities. A model of the natural Fabry–Pérot microcavity is schematically drawn in the inset.

Some fine structures were also observed in the emission spectra of the *P* line, as shown in the inset of Fig. 3, which look very much like the cavity modes of the Fabry–Pérot étalon. Because the PL spectra show the emission actions of many ZnO microrods with different sizes, the sharp lines in the spectra are not regularly spaced.

Figure 5 shows the emission spectra of a single ZnO rod with a 25 μm diam under different excitation densities. It is just the same as in Fig. 3. At low excitation density the free exciton emission is strong in the spectra. A new emission band is presented at the shoulder of the E_{ex} band, which is also considered to be the *P* band. When the rod is excited with a high excitation density, the *P* band is dominant in the spectra. And, the regularly spaced sharp lines can be seen clearly in the spectra. The line spacing is 14 meV. An equation $\Delta E = (\pi ch/L)(n + Edn/dE)^{-1}$ is used to calculated for

the Fabry–Pérot cavity length L, where the Edn/dE is the variation of the refractive index n with photon energy E.[8] The data of the refractive index $n(E)$ are obtained from Ref. 18. The 14 meV mode spacing corresponds to a cavity length of around 21 μm calculated by the above equation, which agrees well with the diameter of the ZnO rod. And, when the rod was turned to another angle along the c axis, the fine structures could not be found in the spectra under the same excitation intensity. (Because we did not have some adjustors on hand to finely measure the angle, we did not know the accurate angle to which we turned.)

Based on the above experiment, it is proposed that the optical cavity is formed by the (1100) facets of the ZnO rod, as schematically shown in the inset of the Fig. 5. Within the excitation region, the high density of excitons is created in the ZnO rod by the photoexcitation and leads to a decrease of the refractive index because of the exciton phase space filling effect. Because the density of excitons is so high, the exciton–exciton collision process occurs, which leads to the emission photoenergy redshift. Due to the mode selective rule of the Fabry–Pérot cavity, regularly spaced sharp lines could be obtained in the spectra.

IV. CONCLUSION

In conclusion, ZnO microrods were fabricated by a simple method. And, the P emission band due to the exciton–exciton scattering process is observed under low excitation intensity at room temperature. The regularly spaced fine structure could also be seen clearly on a single microrod in the PL spectra, which is due to the Fabry–Pérot cavity modes.

ACKNOWLEDGMENTS

This work is supported by the Program of CAS Hundred Talents, the Innovation Project Item of Chinese Academy of Science, and the National Natural Science Foundation of China.

[1] J. M. Hvam, Phys. Rev. B **4**, 4459 (1971).
[2] H. Huang and S. Kock, Phys. Status Solidi B **82**, 531 (1975).
[3] C. Klingshirn, Adv. Mater. Opt. Electron. **3**, 103 (1994).
[4] C. Klingshirn, Phys. Status Solidi B **71**, 547 (1975).
[5] D. M. Bagnall, Y. F. Chen, Z. Zhu, T. Yao, S. Koyama, M. Y. Shen, and T. Goto, Appl. Phys. Lett. **70**, 2230 (1997).
[6] Z. K. Tang, P. Yu, G. K. L. Wong, M. Kawasaki, A. Ohotomo, H. Koinuma, and Y. Segawa, Solid State Commun. **103**, 459 (1997).
[7] Z. K. Tang, P. Yu, G. K. L. Wong, M. Kawasaki, A. Ohotomo, H. Koinuma, and Y. Segawa, Nonlinear Opt. **18**, 355 (1997).
[8] Z. K. Tang, G. K. L. Wong, P. Yu, M. Kawasaki, A. Ohotomo, H. Koinuma, and Y. Segawa, Appl. Phys. Lett. **72**, 3270 (1998).
[9] D. M. Bagnall, Y. F. Chen, M. Y. Shen, Z. Zhu, T. Goto, and T. Yao, J. Cryst. Growth **184/185**, 605 (1998).
[10] H. Cao, Y. G. Zhao, H. C. Ong, S. T. Ho, J. Y. Dai, J. Y. Wu, and R. P. H. Chang, Appl. Phys. Lett. **73**, 3656 (1998).
[11] H. Cao, Y. G. Zhao, S. T. Ho, E. W. Seelig, Q. H. Wang, and R. P. H. Chang, Phys. Rev. Lett. **82**, 2278 (1999).
[12] H. Cao, J. Y. Xu, E. W. Seelig, and R. P. H. Chang, Appl. Phys. Lett. **76**, 2997 (2000).
[13] M. H. Huang, S. Mao, H. Feick, H. Yan, Y. Wu, H. Kind, E. Weber, R. Russo, and P. Yang, Science **292**, 1897 (2001).
[14] M. H. Huang, Y. Wu, H. Feick, N. Tran, E. Weber, and P. Yang, Adv. Mater. (Weinheim, Ger.) **13**, 113 (2001).
[15] A. Ohtomo, K. Tamura, M. Kawasaki, T. Makino, Y. Segawa, Z. K. Tang, G. K. L. Wong, Y. Matsumoto, and H. Koinuma, Appl. Phys. Lett. **77**, 2204 (2000).
[16] H. D. Sun, T. Makino, N. T. Tuan, Y. Segawa, Z. K. Tang, G. K. L. Wong, M. Kawasaki, A. Ohtomo, K. Tamura, and H. Koinuma, Appl. Phys. Lett. **77**, 4250 (2000).
[17] J. M. Hvam, Phys. Status Solidi B **63**, 511 (1974).
[18] W. L. Bond, J. Appl. Phys. **36**, 1674 (1965).